

Wide dynamic detection range of methane gas based on enhanced cavity absorption spectroscopy

Yu Wang(汪玉), Bo-Kun Ding(丁伯坤), Kun-Yang Wang(王坤阳), Jiao-Xu Mei(梅教旭),Ze-Lin Han(韩泽林), Tu Tan(谈图), and Xiao-Ming Gao(高晓明)

Citation: Chin. Phys. B, 2022, 31 (**4**): 040705. DOI: 10.1088/1674-1056/ac2484
Journal homepage: http://cpb.iphy.ac.cn; http://iopscience.iop.org/cpb

What follows is a list of articles you may be interested in

Design of NO_2 photoacoustic sensor with high reflective mirror based on low power blue diode laser

Hua-Wei Jin(靳华伟), Pin-Hua Xie(谢品华), Ren-Zhi Hu(胡仁志), Chong-Chong Huang(黄崇崇), Chuan Lin(林川), Feng-Yang Wang(王凤阳)

Chin. Phys. B, 2020, 29 (**6**): 060701. DOI: 10.1088/1674-1056/ab8376

Atmospheric N_2O gas detection based on an inter-band cascade laser around 3.939 μm

Chun-Yan Sun(孙春艳), Yuan Cao(曹渊), Jia-Jin Chen(陈家金), Jing-Jing Wang(王静静), Gang Cheng(程刚), Gui-Shi Wang(王贵师), Xiao-Ming Gao(高晓明)

Chin. Phys. B, 2020, 29 (**1**): 010704. DOI: 10.1088/1674-1056/ab5ef6

Daily variation of radon gas and its short-lived progeny concentration near ground level and estimation of aerosol residence time

M Mohery, A M Abdallah, A Ali, S S Baz

Chin. Phys. B, 2016, 25 (**5**): 050701. DOI: 10.1088/1674-1056/25/5/050701

Theoretical analysis of stack gas emission velocity measurement by optical scintillation

Yang Yang, Dong Feng-Zhong, Ni Zhi-Bo, Pang Tao, Zeng Zong-Yong, Wu Bian, Zhang Zhi-Rong

Chin. Phys. B, 2014, 23 (**4**): 040703. DOI: 10.1088/1674-1056/23/4/040703

Cross-interference correction and simultaneous multi-gas analysis based on infrared absorption

Sun You-Wen, Zeng Yi, Liu Wen-Qing, Xie Pin-Hua, Chan Ka-Lok, Li Xian-Xin, Wang Shi-Mei, Huang Shu-Hua

Chin. Phys. B, 2012, 21 (**9**): 090701. DOI: 10.1088/1674-1056/21/9/090701

Wide dynamic detection range of methane gas based on enhanced cavity absorption spectroscopy

Yu Wang(汪玉)[1,2], Bo-Kun Ding(丁伯坤)[1,2], Kun-Yang Wang(王坤阳)[1], Jiao-Xu Mei(梅教旭)[1], Ze-Lin Han(韩泽林)[1,3], Tu Tan(谈图)[1], and Xiao-Ming Gao(高晓明)[1,2,†]

[1] *Anhui Institute of Optics and Fine Mechanics, Hefei Institutes of Physical Science, Chinese Academy of Sciences, Hefei* 230026, *China*
[2] *University of Science and Technology of China, Hefei* 230026, *China*
[3] *Anhui Advanced Spectroscopy Optical-electric S&T Co., Ltd.*

(Received 8 July 2021; revised manuscript received 18 August 2021; accepted manuscript online 8 September 2021)

Integrated cavity output spectroscopy (ICOS) is an effective technique in trace gase detection. The strong absorption due to the long optical path of this method makes it challenging in the application scenes that have large gas concentration fluctuation, especially when the gas concentration is high. In this paper, we demonstrate an extension of the dynamic range of ICOS by using a detuned laser combined with an off-axis integrating cavity. With this, we improve the upper limit of the dynamic detection range from 0.1% (1000 ppm) to 20% of the gas concentration. This method provides a way of using ICOS in the applications with unpredictable gas concentrations such as gas leak detection, ocean acidification, carbon sequestration, etc.

Keywords: integrated cavity output spectroscopy (ICOS), trace gas, wide dynamic detection, absorption positions

PACS: 07.88.+y, 42.87.–d, 33.20.Ea **DOI:** 10.1088/1674-1056/ac2484

1. Introduction

High-sensitivity gas detection techniques are of great interest in many fields from the industrial process to the emission control and pollution monitoring. In the past few decades, there have been numbers of exciting developments on high-sensitivity spectroscopy techniques, such as photoacoustic spectroscopy, ring-down cavity spectroscopy and cavity-enhanced absorption spectroscopy. Each of these methods displays advantages and drawbacks in terms of sensitivity, dynamic range, stability and cost. For instance, the photoacoustic spectroscopy has zero background, good linearity and a wide dynamic response range. However, its sensitivity depends on the laser power, and the response speed is on the order of seconds. The ring-down cavity spectroscopy exhibits a high sensitivity and is insensitive to the laser intensity fluctuations. But it requires fast electronics and high stability of the system. Cavity enhanced absorption spectroscopy (CEAS) is another competitive method in the real applications, owing to its high sensitivity, simple experimental apparatus and ease of operation.

So far, the integrated cavity absorption spectroscopy (ICOS) based on the high reflective mirrors has been widely used in high sensitivity and high-precision trace gases detection. It can be applied to various fields, such as industrial process,[1–3] atmosphere,[4,5] environment[6–8] and human health.[9–11] It also enables many applications for marine exploration,[12,13] aerospace[14] and defense.[15] Different application scenes have different technical requirements. Some applications, such as monitoring the background atmosphere, require both the highest sensitivity and precision. For some other applications, such as gas leak detection and exploring the distribution of the gas hydrate in the methane-rich region, the concentration of target gas can vary over 4–5 orders of magnitude. In this context, both the large dynamic range and the high sensitivity are needed.

To improve the performance of these gas detection techniques, there has been much effort to extend the detection range. In 2009, Li Zhengying *et al.*[16] chose two spectral lines with close frequencies and large differences of line strength to improve the dynamic detection range. In 2016, Li *et al.*[17] proposed a method combining direct absorption and wavelength modulation for uncalibrated trace gas detection, and proved that this can extend the dynamic measurement range of the system. Such a method realized the balance between the measurement range and the accuracy. However, for measuring gases with high concentrations, the long optical path induces a strong absorption of the probing laser and leads to a very weak signal being detectable. As a result, this method has a limited upper bond dynamic detection range, and thus it is challenging to use them for measuring gases with high concentration. To improve the dynamic range of the ring-down cavity absorption spectroscopy, Cui *et al.*[18] studied the relation between the total loss in the cavity and the effective optical path. Based on this, they extended the measurement range by tuning the effective cavity length through cavity detuning. However, due to the difficulty of precisely controlling the cavity detuning, the

†Corresponding author. E-mail: xmgao@aiofm.ac.cn
© 2022 Chinese Physical Society and IOP Publishing Ltd

fluctuation of the cavity length results in a large variation of the measurement results. For this concern, Stowasser *et al.*[19] improved the accuracy of the pressure control in the cavity ring-down spectroscopy and extended the measurement range. But in the real application, the gas concentration is hard to predict, and it is difficult to respond to the large change of the environmental concentration in the real time, which causes a large measurement error due to the fluctuation of the pressure.

In this paper, we propose a method combining an off-axis integrated cavity and a laser that is largely detuned from the absorption peak. This method enables a large dynamic range of the integrated cavity absorption spectroscopy. We extend the upper limit of the measurement range from 0.1% (1000 ppm) to a large dynamic range of 20% gas concentration. This method provides a way for the applications requiring the measurement of the gas concentration with large concentration fluctuations, such as gas leak detection, ocean acidification, carbon sequestration and deep-ocean online exploration of methane hydrate and hydrothermal vents.

2. Principle of ICOS for gas sensing

The basic principle of ICOS is shown in Fig. 1. The device uses a tunable laser and two high-reflectivity mirrors to form a high-finesse Fabry–Perot cavity. The gas sample is filled into the cell of the cavity. To formulate the transmission power, we consider a radiation field $E_{\rm i} = E_0 {\rm e}^{{\rm i}2\pi\nu t}$ of the laser passing through the cavity mirror with a reflectivity of R and transmission of T, where ν is the laser frequency and E_0 is the amplitude. The transmitted light amplitude is obtained from the summation of the beam amplitudes leaving the cavity:[20]

$$\begin{aligned} E_{\rm tr}(\psi) &= E_0 {\rm e}^{-{\rm i}\psi/2} T\left({\rm e}^{-NSLP\phi(\nu)/2} + R{\rm e}^{-{\rm i}\psi}{\rm e}^{-NSLP\phi(\nu)} \right. \\ &\quad \left. + R{\rm e}^{-{\rm i}2\psi}{\rm e}^{-2NSLP\phi(\nu)} + \cdots\right) \\ &= \frac{E_0 T {\rm e}^{-{\rm i}\psi/2}{\rm e}^{-NSLP\phi(\nu)/2}}{1 - R{\rm e}^{-{\rm i}\psi}{\rm e}^{-NSLP\phi(\nu)}}, \end{aligned} \tag{1}$$

where $\psi = 2kL = (4\pi nL)/\lambda$. Here L is the length of the cavity, N is the number density of the target species, P is the pressure and S is the spectral line strength. $\phi(\nu) = (1/\pi)\left[\gamma/\left((\nu-\nu_0)^2+\gamma^2\right)\right]$ is the Lorentzian line shape function, where ν_0 is the resonant frequency, and γ is the linewidth of the cavity. Then the transmission power is given as

$$\begin{aligned} I_{\rm tr}(\psi) &= \lfloor E_{\rm tr}(\psi)\rfloor^2 \\ &= \frac{I_0 T^2 {\rm e}^{-NSLP\phi(\nu)}}{1 + R^2{\rm e}^{-2NSLP\phi(\nu)} - 2R{\rm e}^{-NSLP\phi(\nu)}\cos(\psi)}. \end{aligned}$$

Averaging over ψ leads to

$$I_{\rm tr}(\psi) = \frac{I_0 T^2 {\rm e}^{-NSLP\phi(\nu)}}{1 - R^2{\rm e}^{-2NSLP\phi(\nu)}}. \tag{2}$$

To make the equation concise, we denote $\alpha = SLP\phi(\nu)$. For the low gas concentration condition, where the absorption is weak, $N\alpha \ll 1$, so that ${\rm e}^{-2NSLP\phi(\nu)} \approx 1 - N\alpha$. Equation (2) can be simplified as

$$\begin{aligned} I &\approx \frac{I_0 T^2}{1 - R^2(1 - 2N\alpha)} \\ &= \frac{I_0 T^2}{(1-R^2)\left(1 + 2N\alpha \cdot \dfrac{R^2}{1-R^2}\right)} \\ &\approx \frac{I_0 T^2}{(1-R^2)}\left(1 - 2N\alpha \cdot \frac{R^2}{1-R^2}\right). \end{aligned} \tag{3}$$

Here we denote $b_1 = \left(1-R^2\right)/2\alpha R^2$ and $b_2 = \left(1-R^2\right)^2/2I_0T^2\alpha R^2$ to simplify the formula for ease of fitting with experimental data in Section 4, which gives

$$N \approx b_1 - b_2 I. \tag{4}$$

This formula shows a linear dependence of the output intensity on the gas concentration.

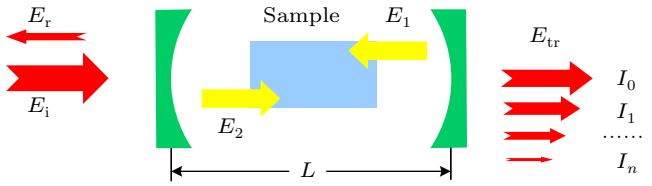


Fig. 1. Illustration of the basic principle of ICOS.

In the non-weak absorption case, the transmitted laser intensity of the integral cavity at the position of the spectral line-wing is given by

$$I = \frac{a_1 {\rm e}^{-a_2 N}}{1 - R^2{\rm e}^{-2a_2 N}}, \tag{5}$$

where

$$\begin{aligned} a_1 &= I_0 T^2, \\ a_2 &= SLP\phi(\nu_{P_1}) = \frac{SLP}{\pi} \cdot \frac{\gamma}{(\nu_{P_2} - \nu_0)^2 + \gamma^2}. \end{aligned}$$

The calibration curve is obtained from Eq. (5),

$$N = \frac{1}{a_2} \ln \frac{2R^2 I}{-a_1 + \sqrt{a_1^2 + 4R^2 I^2}}. \tag{6}$$

In Fig. 2(a), we calculate the absorption spectra in the integrated cavity at different gas concentrations from 2 ppm to 100%. P_1 is located at the center of the absorption peak, and P_2 is chosen to be largely detuned from the absorption peak. The intensity of the transmitted light at the absorption peak P_1 decreases with the increasing gas concentration. At a high concentration, the intensity of the transmitted laser becomes approximately zero and is barely measurable. When the measurement frequency is largely detuned from the absorption

peak, the transmitted laser intensity is much stronger due to the low absorption. Figure 2(b) presents the concentration dependence of the transmitted laser intensity when the gas concentration is low. The results show good linear relationships between the intensity and the concentration with different detunings from the absorption peak. When the gas concentration is high, the transmitted laser intensity shows strong nonlinear relationships to the concentration with different laser detunings from the absorption peak (Fig. 3).

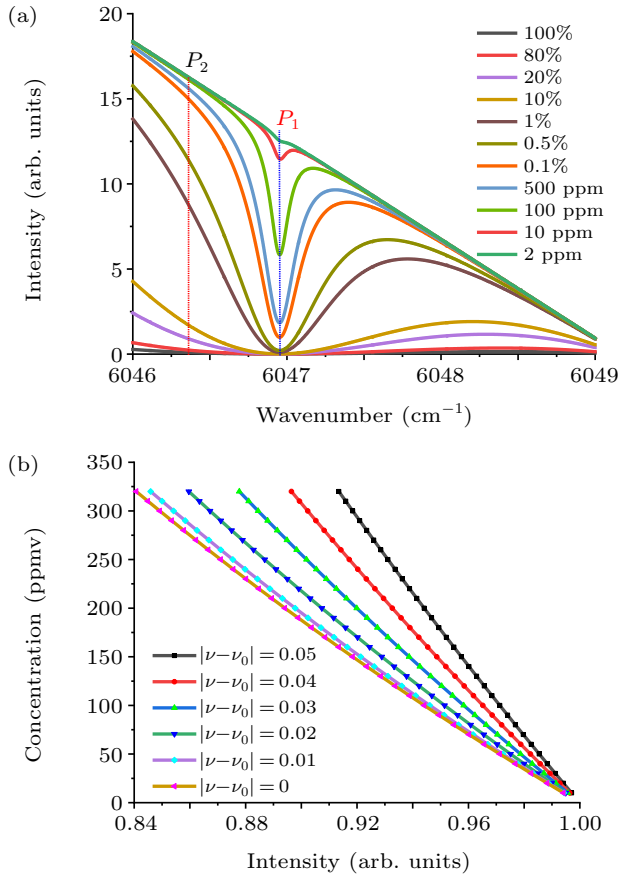


Fig. 2. (a) Simulated absorption spectra of integrated cavity at different gas concentrations; (b) Simulation of the transmitted laser intensity at different positions away from the absorption peak at low gas concentrations.

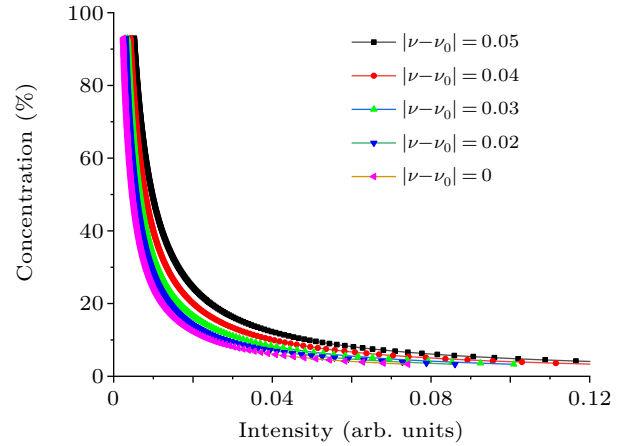


Fig. 3. Simulation of the gas concentration as functions of the transmitted laser intensities in the non-weak absorption case.

3. Experimental setup

The experimental setup is shown in Fig. 4. A 1654 nm InGaAsP distributed feedback (DFB) laser is powered by a high-precision laser controller (LDC 3724, Newport). The injection current is set at 90 mA so that the output power is maintained around 12 mW. We use a sawtooth signal to modulate the on and off of the DFB laser. We first utilize a photodetector to record the laser intensity when the laser is off, and use it as a reference to eliminate the background noise. Then the transmitted laser intensity is measured as the real signal when the laser is on. In order to improve the signal-to-noise ratio, a power adjustable RF white noise source[21] is injected into the DFB semiconductor laser via a bias tee to widen the laser linewidth. The RF noise source power can be adjusted between −40 dBm and −10 dBm to improve the performance of the off-axis integrated cavity instrument with this disturbance. The laser output is collimated by a fiber optical collimator and coupled to an off-axis integrated cavity composed of two lenses with a curvature radius of 1 m and a reflectivity of 99.999%. Two mirrors were placed co-axially on both sides of the optical cavity. The distance between the mirrors is 28 cm and the volume of the cavity was approximately 88 cm^3. The output of the integrated cavity is focused onto an InGaAs detector to measure the laser intensity.

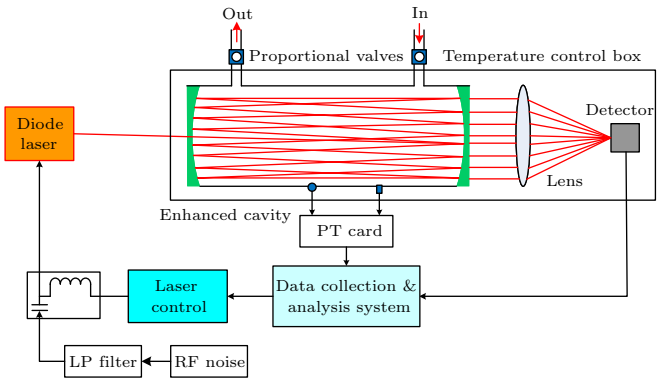


Fig. 4. Experimental schematic of off-axis cavity absorption spectroscopy.

4. Results and analysis

First, we measure the transmission spectra of the off-axis integrated cavity absorption spectroscopy at different concentrations. Figure 5(a) shows the integrated cavity transmission spectra at different gas concentrations from 0.2 ppm to 1 ppm. Figure 5(b) presents the differential signal between intensities at P_1 and P_0 as a function of the concentration, $\Delta I = I_1 - I_0$, where I_1 is the transmitted laser intensity at the absorption peak P_1, and I_0 is the detector dark current at P_0 when the laser is off. By fitting that data to Eq. (4), we obtain the fitting coefficients as $b_1 = 7.96$ W/cm^2 and $b_2 = 10.13$ W/cm^3. The results show a good linear relationship between the transmitted laser intensity and the concentration. The linear correlation R^2

is 99.85%, and the error between the measurement value and calibration curve is $\leq \pm 10\%$.

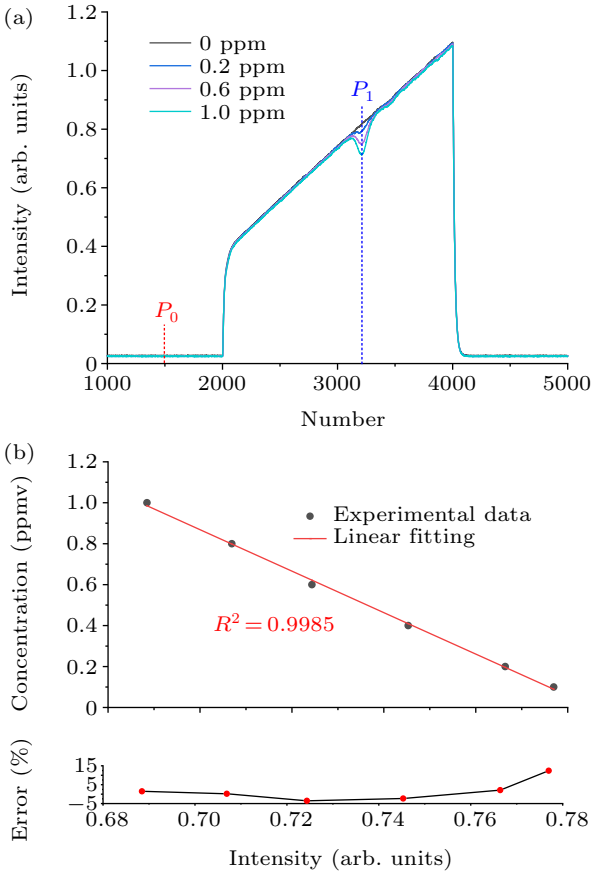


Fig. 5. (a) Plots of the actual output signal of the photon detector. (b) Relation between the gas concentration and the transmission intensity of integrated cavity in the weak absorption case (low concentration).

Figure 6(a) presents the integrated cavity transmission spectrum of the 10 groups of data with concentrations ranging from 1.5 ppm to 20%. The lineshape of the absorption spectroscopy in Fig. 6(a) shows a significant deformation at high gas concentrations. Also, the transmitted laser intensity at the absorption peaks is approximately zero at high concentrations. Therefore, it is hard to use the absorption depth at or close to the absorption peak to determine the gas concentration. In this case, we utilize a laser that is largely detuned from the absorption peak to decrease the absorption intensity. This method helps avoid the absorption saturation and extends the upper limit of the dynamic range of the integrated cavity absorption spectroscopy. Figure 6(b) shows the experimental results of the transmitted laser intensity as a function of the gas concentration when the laser is set to be far off-resonant from the absorption peak. Here we compare the results at four different positions of the output signal of the photon detector (number 3200, 3400, 3650, and 3800). When the laser wavenumbers are very close to the absorption peak, the transmitted laser intensity dramatically drops to approximately zero with an increasing gas concentration, and then stays unchanged around zero within a large concentration scale. Therefore, the intensities at different gas concentrations cannot be distinguished due to the saturated absorption. In contrast, when the laser is detuned far away from the absorption peak, the transmitted laser intensity decreases slowly with an increase gas concentration. This enables the precise measurement of the absorption to determine the gas concentration. Therefore, by choosing a proper laser frequency, we are able to measure both high and low gas concentrations.

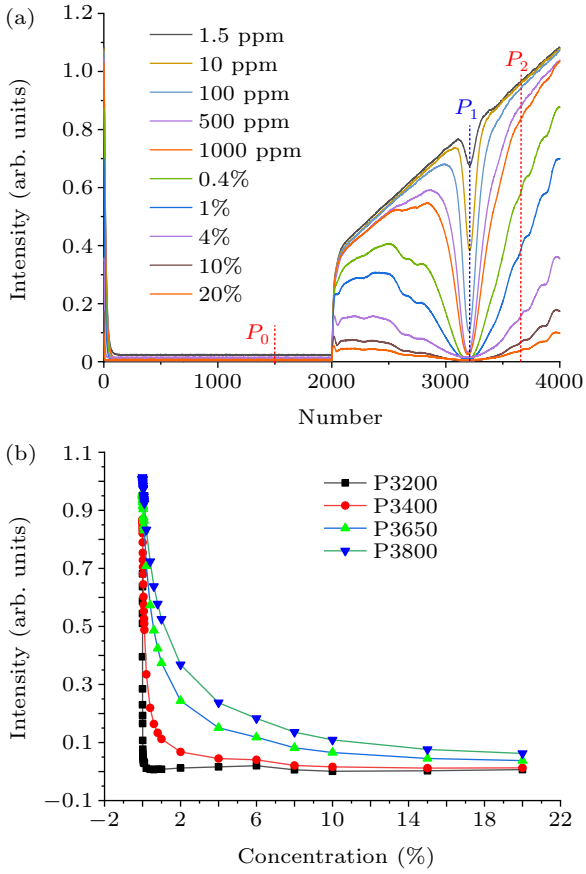


Fig. 6. (a) Plots of the actual output signal of the photon detector. (b) The variation curve of the transmitted laser intensity with concentration (high concentration) at different positions away from the absorption peak of the integrated cavity.

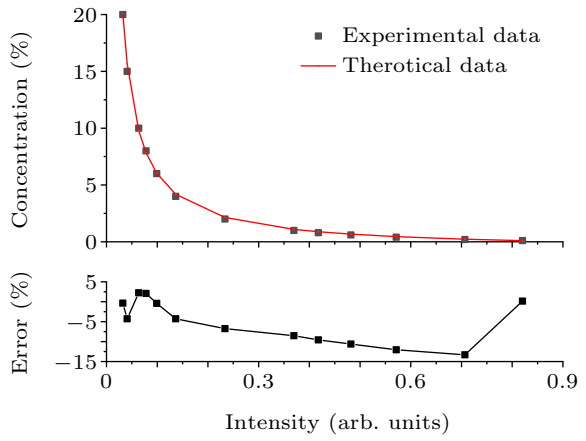


Fig. 7. The gas concentration as a function of the transmitted laser intensity of the integrated cavity. The laser frequency is set to be far away from the absorption peak.

Figure 7 shows experimental results of the transmitted laser intensity as a function of the concentration. The actual

output signal intensity of the photon detector is acquired at the positions that is 450 numbers detuned from the absorption peak. The data fits well to Eq. (5), which gives the coefficients a_1 and a_2 as 1.87×10^{-5} W/cm^2 and 1.4×10^{-5} cm^{-3}, respectively. The deviation between the experimental value and theoretical calibration is within $\pm 10\%$. Therefore, the gas concentrations can be measured with a high precision in a large dynamic range.

5. Conclusion

Gas detection with a large dynamic range has extensive applications in various fields, such as industry, environment, etc. We propose and experimentally demonstrate a method that can extend the dynamic range of the off-axis integrated cavity output spectroscopy. Such a method extends the upper limit of the dynamic detection range from 0.1% (1000 ppm) to 20% concentrations. With a low gas concentration, the system shows a good linear response. At a high gas concentration, a largely detuned laser is chosen to decrease the absorption intensity. This enables the precise quantitative measurement of the gas concentration in a large dynamic range, with a less than 10% uncertainty. Our results meet the requirements of natural gas detection and other industrial applications.

Acknowledgments

Project supported by the National Key Research and Development Program of China (Grant No. 2017YFC0209700) and the National Natural Science Foundation of China (Grant No. 41730103).

References

[1] Le L D, Tate J D, Seasholtz M B, Gupta M, Owano T, Baer D, Knittel T, Cowie A and Zhu J 2008 *Appl. Spectrosc.* **62** 59

[2] Zheng K Y, Zheng C T, Yao D, Hu L E, Liu Z D, Li Y H, Zhang Y, Wang Y D and Tittel F K 2019 *Analyst* **144** 2003

[3] Centeno R, Mandon J, Cristescu S M and Harren F J M 2014 *Sensor. Actuat. B-Chem.* **203** 311

[4] Wang K Y, Shao L G, Chen J J, Wang G S and Gao X M 2020 *Sensors* **20** 6192

[5] Wang J J, Tian X, Dong Y, Chen J J, Tan T, Zhu G D, Chen W D and Gao X M 2019 *Opt. Lett.* **44** 3298

[6] Kaul D S, Zhi N, Westerdahl D, Yin X and Cary R A 2016 *Aerosol Air Qual. Res.* **16** 1345

[7] Mahesh P, Sreenivas G, Rao P, Dadhwal V K, Krishna S and Mallikarjun K 2015 *Int. J. Remote Sens.* **36** 5754

[8] Sayres D S, Moyer E J, Hanisco T F, Clair J M S, Keutsch F N, O'Brien A, Allen N T, Lapson L, Demusz J N, Rivero M, Martin T, Greenberg M, Tuozzolo C, Engel G S, Kroll J H, Paul J B and Anderson J G 2009 *Rev. Sci. Instrum.* **80** 044102

[9] Silva M L, Sonnenfroh D M, Rosen D I, Allen M G and Keefe A O 2005 *Appl. Phys. B* **81** 705

[10] Bakhirkin Y A, Kosterev A A, Curl R F, Tittel F K, Yarekha D A, Hvozdara L, Giovannini M and Faist J 2006 *Appl. Phys. B* **82** 149

[11] Pal M, Bhattacharya S, Maity A, Chaudhuri S and Pradhan M 2020 *Anal. Chem.* **92** 5717

[12] Wankel S D, Huang Y W, Gupta M, Provencal R and Girguis P R 2012 *Environ. Sci. Technol.* **47** 1478

[13] Gonzalez-Valencia R, Magana-Rodriguez F, Gerardo-Nieto O, Sepulveda-Jauregui A, Martinez-Cruz K, Walter-Anthony K, Baer D and Thalasso F 2014 *Environ. Sci. Technol.* **48** 11421

[14] Rodin A, Vinogradov I, Zenevich S, Spiridonov M, Gazizov I, Kazakov V, Meshcherinov V, Golovin I, Kozlova T, Lebedev Y, Malashevich S, Nosov A, Roste O, Venkstern A, Klimchuk A, Semenov V, Barke V, Durry G, Ghysels-Dubois M, Tepteeva E and Korablev O 2020 *Appl. Sci.* **10** 2

[15] Arslanov D D, Cristescu S M and Harren F 2010 *Opt. Lett.* **35** 3300

[16] Li Z Y and Wang H H 2009 *Journal of Wuhan University of Technology* **31** 42

[17] Li J S, Deng H, Sun J, Yu B L and Fischer H 2016 *Sensor. Actuat. B* **231** 723

[18] Cui H, Li B C, Han Y L, Wang J, Gao C and Wang Y F 2016 *Opt. Express* **24** 13343

[19] Stowasser C, Farinas A D, Ware J, Wistisen D W, Rella C, Wahl E, Crosson E and Blunier T 2014 *Appl. Phys. B* **116** 255

[20] Zybin A, Kuritsyn Y A, Mironenko V R and Niemax K 2004 *Appl. Phys. B* **78** 103

[21] Ciaffoni L, Couper J, Hancock G, Peverall R, Robbins P A and Ritchie G A D 2014 *Opt. Express* **22** 17030